



Fabrication and characterization of multimode optical fiber sensor for chemical temperature monitoring using optical time domain reflectometer

Marwan Hafeedh Younus ^{a,b}, Odai Falah Ameen ^{a,b}, Norizah Redzuan ^c,
Norhayati Ahmad ^c, Raja Kamarulzaman Raja Ibrahim ^{a,*}

^a Laser Center, Physics Department, Faculty of Science, Universiti Teknologi Malaysia (UTM), 81310 Johor Bahru, Johor, Malaysia

^b Department of Physics, Faculty of Education, University of Mosul, 41002 Mosul, Iraq

^c Department of Material, Manufacturing and Industrial Engineering, Faculty of Mechanical Engineering, Universiti Teknologi Malaysia (UTM), 81310 Johor Bahru, Johor, Malaysia

Received 13 August 2017; revised 20 November 2017; accepted 4 December 2017

Available online 21 December 2017

Abstract

In this work, the optical fiber sensor system to measure the optical loss due to temperature variation of gasoline and toluene was papered. The optical fiber sensor was characterized using optical time domain reflectometer (OTDR). The sensor was a 50 cm multimode fiber with about 1–3 cm at its central region being partially unclad. The partial uncladding was carried out using chemical etching technique. The optical loss of sensor was measured when unclad part exposed to gasoline and toluene respectively at different temperature ranging from 25 °C to 60 °C. The optical loss of sensor increases in a step drop of OTDR trace as the temperature is increased. The rate of optical loss was estimated to be 0.01576 dB/°C and 0.02212 dB/°C for gasoline and toluene respectively.

© 2017 The Authors. Production and hosting by Elsevier B.V. on behalf of University of Kerbala. This is an open access article under the CC BY-NC-ND license (<http://creativecommons.org/licenses/by-nc-nd/4.0/>).

Keywords: Optical fiber temperature sensor; Optical fiber chemical sensor; OTDR

1. Introduction

Many material properties show strong temperature dependence, for examples density, electrical conductivity, refractive index, rigidity and diffusion [1,2].

Most of temperature dependence measurement tasks in industrial applications and the research can be carried out using conventional electric temperature sensors such as, thermocouples, junction temperature sensors, resistance temperature detectors or thermistors [2,3]. Despite the spreading of electrical sensors, their usage is impractical, if not entirely impossible in certain types of applications such as, chemical plants, landfills, chemical delivery pipelines, water ductworks, and similar applications. These types of sensors are

* Corresponding author.

E-mail addresses: marwan.hafed@yahoo.com (M.H. Younus), rkamarulzaman@utm.my (R.K. Raja Ibrahim).

Peer review under responsibility of University of Kerbala.

susceptible to corrosive attacks and sensitive to various sources of error caused, for example, by electromagnetic interference [4,5]. Optical fiber sensors present clear advantages for operation in such extreme conditions. It can be used for remote measurements in environments which are hazardous or which suffer from the electromagnetic interference [6,7]. An optical fiber can act as the sensing element for a large variety of external parameters such as strain [8], temperature [9] and pressure [10], because it is able to survive to the harsh environmental constraints. Different classes of fiber-based sensors have been investigated, such as Fiber Bragg Gratings (FBGs) [11], Brillouin [12], Raman [13], Rayleigh scattering based techniques for distributed measurements [10], Mach-Zehnder interferometer sensors [14] and fiber surface plasmon resonance sensors [15]. The optical fiber sensors are categorized as either intensity or interferometric sensors. There are other optical techniques based on light scattering such as, radioactive losses [16], reflectance changes [17] and magneto-optic [18]. However the optical fiber sensor system must improve the performances for the temperature monitoring in the fields that depend on the temperature in their work such as generation of nuclear power reactors, spent-fuel pools and industries [2,19,20]. Moreover, other highly sensitive techniques were used for temperature monitoring such as, bandgap hybrid structures, polymer optical fibers, solid core photonic crystal fiber and hollow core photonic crystal fiber [21–25]. Of late, interest has turned to distributed fiber sensors, which enable the temperature to be monitored at many independent positions along fiber and thus to determine the thermal distribution and the location of hot spots. The first implementation of a distributed temperature sensor relied on optical time-domain reflectometry OTDR principle, invented by Barnoski and Jensen in 1976, which was the first method for distributed fiber measurements using backward Rayleigh scattering to determine the optical loss along fibers [26,27]. In such fibers, a localized temperature rise results in an increased scattering signal which may be detected and located by OTDR. Additionally, the OTDR enables to monitor the temperature profile along the length of a fiber continuously with a good response time and spatial resolution [28–31].

In this work, a multi-mode optical fiber (MMF) was used to demonstrate chemical temperature sensing. The sensor was fabricated by conventional chemical etching method using hydrofluoric acid (HF). An optical time domain reflectometer (OTDR) is used to determine the backscattering losses.

2. Theory of OTDR operation

In this study the (MW9070B) Optical Time Domain Reflectometer (OTDR) was used. It can be used to measure total loss, interval loss, splice loss and length of fiber. The main components of a conventional OTDR are laser diode (LD), detector avalanche photo diode (APD), an analog digital converter and a digital processor. The LD launch pulse light with low repetition into the fiber under test. Backscattered light is generated by Rayleigh scattering and Fresnel reflection in the fiber. The backscattered signals are introduced into the APD via a directional fiber coupler and averaged to improve the signal to noise ratio (SNR). Some of the light, thus scattered is guided by the fiber back to the launching end where it is detected by the receiver as shown in Fig. 1. The device operates at 1300 nm wavelengths with the pulse width range varied between 20 and 500 ns. The OTDR had the maximum dynamic range up to 50 dB and the average scan speed 150 s.

The resulting waveform in the OTDR device takes the shape of a decaying pulse since the forward-traveling pulse and that portion of the light which is scattered backwards are both attenuated by propagation along the fiber. Fig. 2 shows the whole trace of OTDR includes the splicing loss, connector reflection and Fresnel reflection. However, the scattered power $p(t)$ returning to the launching end after time t is given by equation (1) [31–33]

$$p(t) = p_0 W \eta_{(z)} \exp - \left[\int_0^t \alpha_{(z)} V_g \right] \quad (1)$$

where p_0 is the power launched into the fiber, W is the pulse width, V_g is the group velocity, $\alpha_{(z)}$ is the local attenuation coefficient and $\eta_{(z)}$ is the backscatter factor. Also, the distance z from the launching end is related to elapsed time t via equation (2) [31–33]

$$z = \frac{V_g t}{2} \quad (2)$$

3. Methods of fabrication MMF sensor and experimental setup

A 50 cm silica MMF with its core and cladding of diameters 50 and 125 μm respectively and RI of 1.41 was used. The gasoline and toluene with refractive indices 1.39 and 1.4961 respectively were used as samples to be detected by the sensor. A 1–3 cm length around the central region of the MMF was mechanically

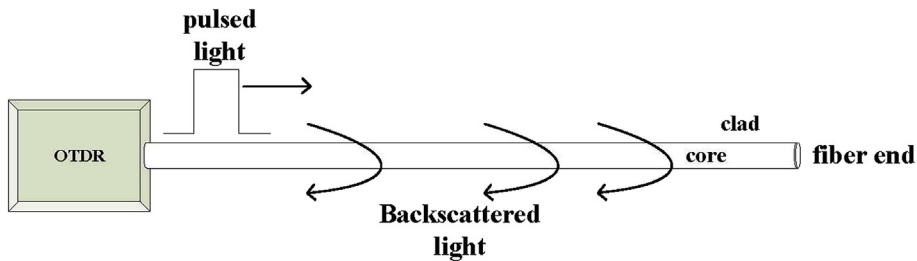


Fig. 1. Optical time domain reflectometry principle.

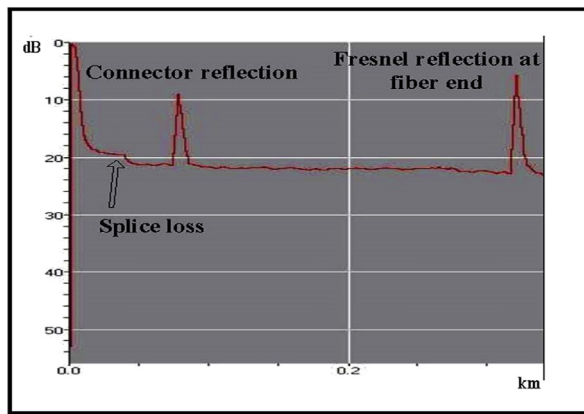


Fig. 2. OTDR trace attenuation includes the splicing loss, connector loss and Fresnel reflection.

stripped and cleaned with isopropyl alcohol and deionized water prior to etching. Then, the cladding of MMF was etched using HF acid with concentration equal to 49%. The MMF was then mounted tightly on HF-plastic resistant, and then it immersed into the HF solution (HF-Panreac AppliChem, Spain) at room temperature around 25 °C. When etching time were 5 min, 10 min, 15 min and 20 min, the diameter was found to be 107 µm, 89 µm, 61 µm and 50 µm respectively. Then, 50 µm core diameter fibers were prepared by removing all cladding for 20 min etching time. After dissolved the cladding, the MMF was raised from HF solution and dipped into isopropyl alcohol, deionized water and followed by drying with dust free tissues to remove any remaining HF from the fiber surface. The image of the electron microscope of the MMF sensor before and after immersed in HF acid is shown in Fig. 3. It can see the whole cladding of the MMF sensor found to be removed. Besides, the results showed that the diameter of the clad was reduced in a roughly linear form with etching time rate $\sim -3.98 \mu\text{m}/\text{min}$ as shown in Fig. 4. It can be seen that by 20 min of etching the diameter of the MMF

decreased and its cladding has completely dissolved in the HF (see Fig. 4). Furthermore, the diameter size of the MMF sensor reduced from 125 µm to 50 µm, which mean that the cladding layer was removed without any damage to the core surface. However, if the time etching was more than the 20 min, the core fiber is found to dissolve and this set the limit of detection sensitivity by means of etching.

4. Experimental setup

The experimental setup for temperature monitoring based MMF sensors with OTDR detector is shown in Fig. 5.

In this study, the system detection consists of a MMF worked as the sensing element and an OTDR as analyzer. The ends of the MMF sensor are required to be perfectly flat and perpendicular to the axis in order to reduce the splicing losses. The MMF sensor connected by means of a fusion splicer to the 150 m of Multimode launch fiber (MMF50C 0.20 NA) and 150 m Multimode receive fiber (MMF50C 0.20 NA). All the MMF used has the same core diameter of 50 µm to reduce the losses due to the core mismatched. The optical fiber sensor system was connected to an OTDR at one end to obtain the OTDR trace while the other end exposed to air. The optical loss is determined a drop step in the OTDR trace as shown in Fig. 6.

Additionally, the OTDR trace of MMF sensor before the clad is etched was recorded and use as a reference trace. Then, the MMF sensor was etched and immersed into sample and again the OTDR trace was recorded. Then the return loss was recorded as a different of the both traces of the OTDR at various temperature ranging from 25 °C to 60 °C (see Fig. 6). To measure the temperature, the sensor was placed in a controlled heater with thermocouple to monitor the temperature variation of chemical liquids (see Fig. 5).

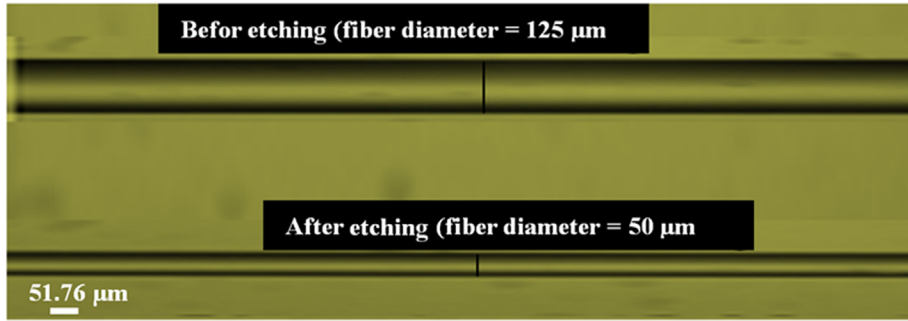


Fig. 3. Electron microscopic image of MMF sensor (before and after 20 min etching).

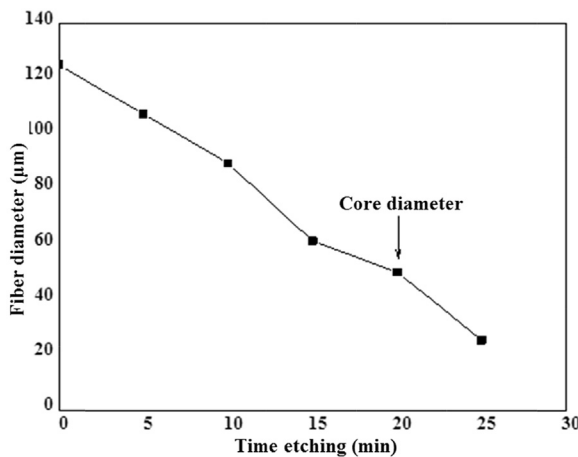


Fig. 4. The MMF sensor diameter against the etching time.

5. Results and discussion

5.1. Chemical leakage monitoring using MMF sensor

Fig. 7 shows the OTDR trace for gasoline and toluene with 1 cm unclad portion of 50 cm MMF sensor. The bare core of the sensor was in direct contact with the chemicals of different the refractive index. The guided modes of the source signals were affected,

changed to evanescent-wave and escaped out from the fiber core thereby decreasing the intensity of light inside the fiber. The total optical losses in this work, of gasoline and toluene were found to be 1.823 dB and 1.922 dB respectively, while the loss without any chemical (air) was 1.560 dB. Moreover, the optical return loss seemed to be dependent on the refractive index of the chemicals. From the results it seemed that the higher the refractive index of the chemical the more will be the loss. Additionally, the amount of the optical loss showed almost linear behavior with respect to the refractive index of chemicals as plotted in Fig. 8.

Fig. 9 shows the optical return loss versus the length of the MMF sensor in toluene condition. The experiments were performed on the unclad part by chemically etched its cladding in the following portion of the fiber of lengths: 1, 2 and 3 cm. The unclad part of MMF sensor was exposed to toluene, and the optical return loss was found to be proportional linearly to the MMF sensor length which is obtained and recorded using OTDR. It can be noted that the optical return loss associated with sensing length clearly increased as the length of sensor is increased and was found to be 30.8 dB/m. From this result it can be deduced that the amount of escaping light depends on the unclad length of the sensor part. The increased length of the

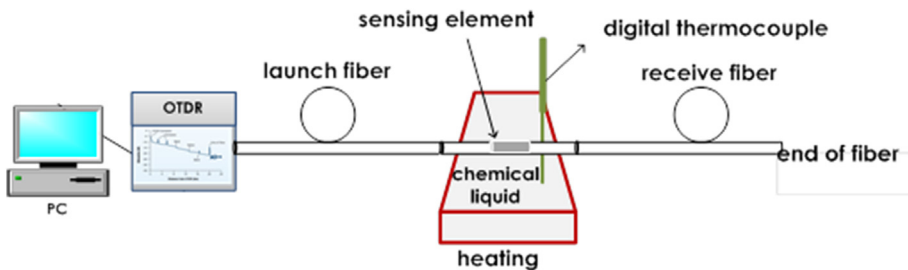


Fig. 5. The setup for temperature measurement using the MMF sensor.

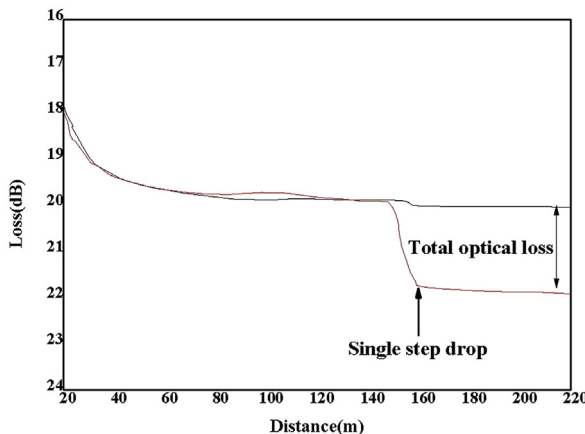


Fig. 6. OTDR trace attenuation showing the splicing loss, connector loss and Fresnel reflection.

interaction region with chemical results in an increased attenuation or and increased Rayleigh scattering, which can both be measured by standard OTDR. Moreover, this attenuation causes the decreases in the light propagating at MMF sensor region, and thus increases the loss which is finally enhance the sensitivity of the system detection.

5.2. The effect of the temperature variation of chemicals liquids on the sensor response

Figs. 10 and 11 depicted the typical traces of the OTDR measurement for 1 cm length of the MMF sensor in different temperature of gasoline and toluene respectively. The temperature of gasoline and toluene was varied from 25 °C to 60 °C creating a non-

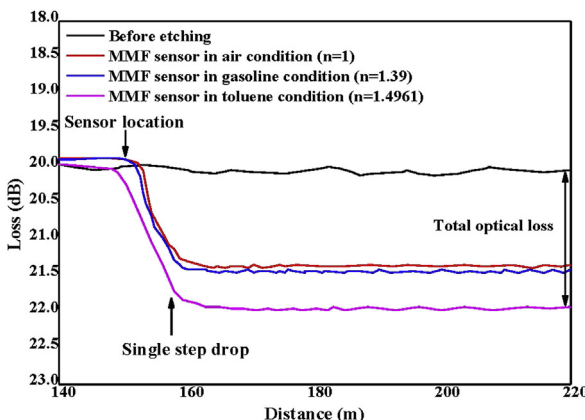


Fig. 7. The typical OTDR trace before etching and after 20 min etching 1 cm of unclad length of MMF sensor. The unclad part was exposed successively to gasoline and toluene.

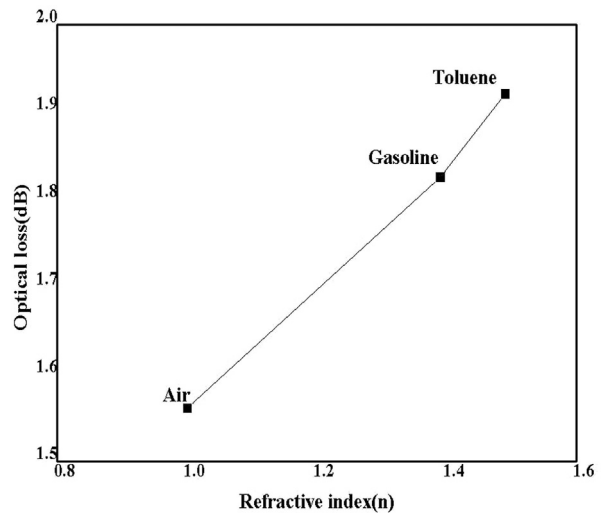


Fig. 8. The total optical loss versus refractive index (air, gasoline and toluene).

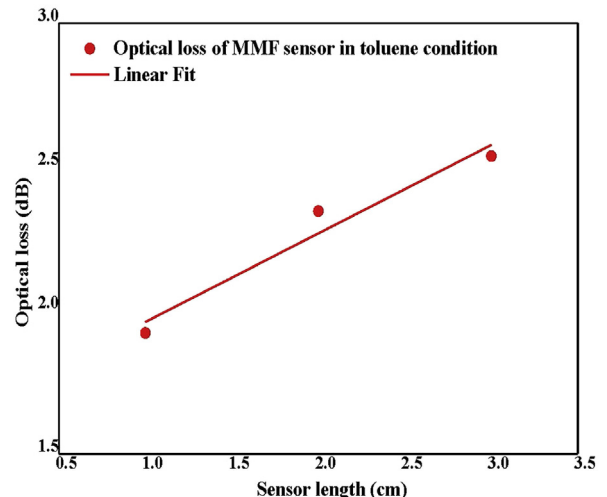


Fig. 9. The return loss versus different length of the MMF sensor immersed in toluene.

reflective event on the sensor. The optical losses induced by rise the temperature of gasoline and toluene recorded as the step drop in the OTDR trace. The temperature variation induces the total loss relative of 1.973 dB and 2.682 dB of gasoline and toluene respectively. It is clear that the optical return loss is directly related to the local temperature variation of chemicals. Moreover, the increase of the temperature at the MMF sensor region is one of the responsible causes for light scattering and then part of the optical signal transfer to the surrounding medium.

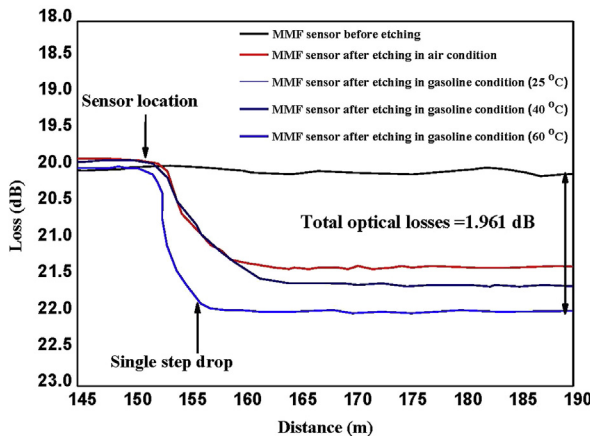


Fig. 10. The typical OTDR trace of MMF sensor response with unclad length 1 cm to temperature variation of gasoline condition.

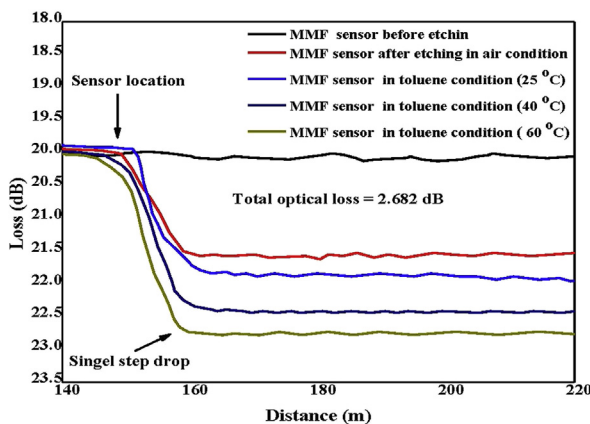


Fig. 11. The typical OTDR trace of MMF sensor response with unclad length 1 cm to temperature variation of toluene condition.

The results were further analyzed to obtain the optical loss of gasoline and toluene versus temperature variation plotted in Fig. 12. The optical loss rates of gasoline and toluene were estimated to be $\sim 0.016 \text{ dB}/\text{°C}$ and $\sim 0.022 \text{ dB}/\text{°C}$ respectively.

It seemed that the loss increased linearly with temperature; indicating the amount of light coupled out of the fiber core increases more rapidly with increase the temperature. It can see from Fig. 12 that the loss of toluene is larger than the loss of gasoline about 0.709 dB because the toluene it has refractive index larger the refractive index of gasoline. Additionally, the temperature variation of chemicals induced some changes in optical behavior leading to loss some of light in MMF sensor at unclad part. Overall, the results show that the optical fiber chemical sensor system includes the MMF sensor and OTDR has potential for

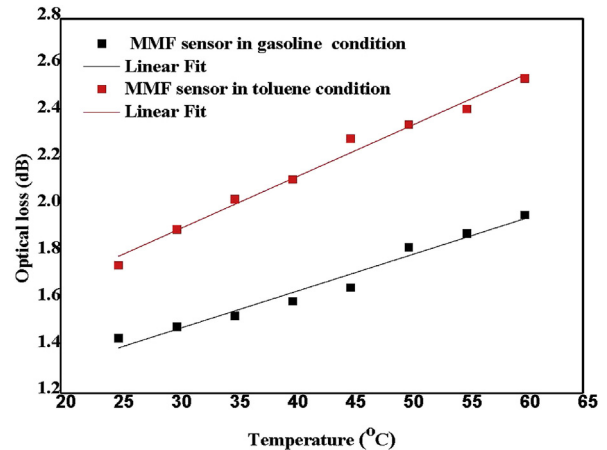


Fig. 12. Total optical loss versus the temperature variation of gasoline and toluene for 1 cm sensor.

temperature monitoring, and they are able to localize the change in the temperature at unclad part.

6. Conclusion

The optical fiber sensor system was implemented in this study using an OTDR as analyzer and MMF as the sensor element. Based on the evanescent wave mode principle, the sensor preparation involved the removal of a portion of the cladding of the MMF. The length of cladding removed was 1, 2 and 3 cm using chemical etching method. The configuration of sensor system was capable of responding at different refractive index of the detected chemical. It was also able to be used to monitor the temperature variation of gasoline and toluene. The measurement of temperature ranging from 25 °C to 60 °C was achieved with good linearity. The results were further analyzed to obtain the total loss associated with gasoline and toluene due to temperature variation and estimated to be 1.973 and 2.682 dB with optical losses rate $\sim 0.016 \text{ dB}/\text{°C}$ and $\sim 0.022 \text{ dB}/\text{°C}$ respectively. The results show a good response of MMF sensor using a commercial OTDR for a range of temperature sensor applications.

Acknowledgment

The authors want to thank and appreciate the staff at the Laser Center, University Technology Malaysia (UTM) for providing research facilities required to complete this study. The authors gratefully acknowledge for financial support research of Grant No. 4F648. Marwan is grateful to the Ministry of Higher Education and Scientific Research, Iraq for providing PhD scholarship.

References

- [1] E. Udd, Fiber Optic Sensors, SPIE Optical Engineering Press, Wiley Online Library, 1993.
- [2] L. Hoffmann, M.S. Müller, S. Krämer, M. Giebel, G. Schwotzer, T. Wieduwilt, Applications of fibre optic temperature measurement, *Proc. Estonian Acad. Sci. Eng.* 13 (2007) 363–378.
- [3] K.V. Rai, Temperature sensors and optical sensors, *Appl. Phys. B* 88 (2007) 297–303.
- [4] K. Hix, Leak Detection for Landfill Liners Overview of Tools for Vadose Zone Monitoring, DIANE Publishing, 1998.
- [5] R. Noyes, Handbook of Leak, Spill, and Accidental Release Prevention Techniques, William Andrew Publishing, 1992.
- [6] S. Rizzolo, E. Marin, A. Boukenter, Y. Ouerdane, M. Cannas, J. Perisse, et al., Radiation hardened optical frequency domain reflectometry distributed temperature fiber-based sensors, *IEEE Trans. Nucl. Sci.* 62 (2015) 2988–2994.
- [7] S. Girard, J. Kuhnhenn, A. Gusarov, B. Brichard, M. Van Uffelen, Y. Ouerdane, et al., Radiation effects on silica-based optical fibers: recent advances and future challenges, *IEEE Trans. Nucl. Sci.* 60 (2013) 2015–2036.
- [8] B.L. Martins, J.B. Kosmatka, Evaluation of fiber optic strain sensors for applications in structural health monitoring, in: 57th AIAA/ASCE/AHS/ASC Structures, Structural Dynamics, and Materials Conference, 2016, pp. 708–715.
- [9] N. Jing, C. Teng, F. Yu, G. Wang, J. Zheng, Temperature dependence of a refractive index sensor based on side-polished macrobending plastic optical fiber, *IEEE Sens. J.* 16 (2016) 355–358.
- [10] Z. Yizheng, W. Anbo, Miniature fiber-optic pressure sensor, *IEEE Photon. Technol. Lett.* 17 (2005) 447–449.
- [11] G. Pereira, M. McGugan, L.P. Mikkelsen, Method for independent strain and temperature measurement in polymeric tensile test specimen using embedded FBG sensors, *Polym. Test.* 50 (2016) 125–134.
- [12] Y. Bao, G. Chen, Temperature-dependent strain and temperature sensitivities of fused silica single mode fiber sensors with pulse pre-pump Brillouin optical time domain analysis, *Meas. Sci. Technol.* 27 (2016) 065101.
- [13] C. Cangialosi, Y. Ouerdane, S. Girard, A. Boukenter, S. Delepine-Lesoille, J. Bertrand, et al., Development of a temperature distributed monitoring system based on Raman scattering in harsh environment, *IEEE Trans. Nucl. Sci.* 61 (2014) 3315–3322.
- [14] J. Harris, P. Lu, H. Larocque, L. Chen, X. Bao, In-fiber Mach-Zehnder interferometric refractive index sensors with guided and leaky modes, *Sensor Actuator B Chem.* 206 (2015) 246–251.
- [15] L.C.C. Coelho, J.M.M.M. de Almeida, H. Moayyed, J.L. Santos, D. Viegas, Multiplexing of surface plasmon resonance sensing devices on etched single-mode fiber, *J. Lightwave Technol.* 33 (2015) 432–438.
- [16] Y. Koyamada, Numerical analysis of core-mode to radiation-mode coupling in long-period fiber gratings, *IEEE Photon. Technol. Lett.* 13 (2001) 308–310.
- [17] G. Gagliardi, M. Salza, P. Ferraro, E. Chehura, R.P. Tatam, T.K. Gangopadhyay, et al., Optical fiber sensing based on reflection laser spectroscopy, *Sensors* 10 (2010) 1823–1845.
- [18] T. Shen, Y. Feng, B. Sun, X. Wei, Magnetic field sensor using the fiber loop ring-down technique and an etched fiber coated with magnetic fluid, *Appl. Opt.* 55 (2016) 673–678.
- [19] Z. Li, Y. Wang, C. Liao, S. Liu, J. Zhou, X. Zhong, et al., Temperature-insensitive refractive index sensor based on in-fiber Michelson interferometer, *Sensor Actuator B Chem.* 199 (2014) 31–35.
- [20] B. De Pauw, A. Lamberti, J. Ertveldt, A. Rezayat, S. Vanlanduit, K. Van Tichelen, et al., Temperature monitoring using fibre optic sensors in a lead-bismuth eutectic cooled nuclear fuel assembly, *Nucl. Eng. Des.* 297 (2016) 54–59.
- [21] G. Woyessa, A. Fasano, C. Markos, H.K. Rasmussen, O. Bang, Low loss polycarbonate polymer optical fiber for high temperature FBG humidity sensing, *IEEE Photon. Technol. Lett.* 29 (2017) 575–578.
- [22] C. Markos, Thermo-tunable hybrid photonic crystal fiber based on solution-processed chalcogenide glass nanolayers, *Sci. Rep.* 6 (2016) 31711.
- [23] S. Shabahang, N.S. Nye, C. Markos, D.N. Christodoulides, A.F. Abouraddy, Reconfigurable opto-thermal graded-index waveguiding in bulk chalcogenide glasses, *Optic Lett.* 42 (2017) 1919–1922.
- [24] C. Markos, K. Vlachos, G. Kakarantzas, Guiding and Birefringent Properties of a Hybrid PDMS/silica Photonic Crystal Fiber, *SPIE LASE*, SPIE, 2011, p. 6;
- [25] E. Brinkmeyer, Analysis of the backscattering method for single-mode optical fibers, *J. Opt. Soc. Am.* 70 (1980) 1010–1012.
- [26] C. Markos, G. Antonopoulos, G. Kakarantzas, Broadband guidance in a hollow-core photonic crystal fiber with polymer-filled cladding, *IEEE Photon. Technol. Lett.* 25 (2013) 2003–2006.
- [27] M.K. Barnoski, S.M. Jensen, Fiber waveguides: a novel technique for investigating attenuation characteristics, *Appl. Opt.* 15 (1976) 2112–2115.
- [28] A.J. Rogers, Polarization-optical time domain reflectometry: a technique for the measurement of field distributions, *Appl. Opt.* 20 (1981) 1060–1074.
- [29] L. Palmieri, L. Schenato, Distributed optical fiber sensing based on Rayleigh scattering, *Open Opt. J.* 7 (2013).
- [30] J. Buerck, S. Roth, K. Kraemer, H. Mathieu, OTDR fiber-optical chemical sensor system for detection and location of hydrocarbon leakage, *J. Hazard. Mater.* 102 (2003) 13–28.
- [31] A.H. Hartog, A.P. Leach, M.P. Gold, Distributed temperature sensing in solid-core fibres, *Electron. Lett.* 21 (1985) 1061–1062.
- [32] S. Eich, E. Schmälzlin, H.-G. Löhmansröben, Distributed fiber optical sensing of oxygen with optical time domain reflectometry, *Sensors* 13 (2013) 7170–7183.
- [33] S.D. Personick, Photon probe—an optical-fiber time-domain reflectometer, *Bell Syst. Tech. J.* 56 (1977) 355–366.
- [34] E. Brinkmeyer, Analysis of the backscattering method for single-mode optical fibers, *J. Opt. Soc. Am.* 70 (1980) 1010–1012.